Comet Hale-Bopp (C/1995 O1) Near 2.3 AU Post-Perihelion: SWUIS Measurements of the H_2O and Dust Production

S. Alan Stern, William B. Colwell, Michel C. Festou, Peter M. Tamblyn, Joel Wm. Parker
Southwest Research Institute, Suite 426, 1050 Walnut Street, Boulder, Colorado 80302

David C. Slater
Southwest Research Institute, 6220 Culebra Road, P.O. Drawer 28510, San Antonio, TX 78238

Paul R. Weissman
Jet Propulsion Laboratory, 4800 Oak Grove Drive Pasadena, CA 91109

and

Larry J. Paxton
Applied Physics Laboratory, Johns Hopkins University, 11100 Johns Hopkins Road, Laurel, MD 20723

Received ______________; accepted ______________

Submitted to *The Astronomical Journal*

ABSTRACT

The Southwest Ultraviolet Imaging System (SWUIS) imaged comet C/1995 O1 (Hale-Bopp) in various bandpasses from the Space Shuttle on nine occasions during 1997 August 9–15. These observations occurred when the solar elongation of the comet was too small to permit HST and other UV observations. Here we present some first results of the continuum and gas emission measurements collected by SWUIS. We find that Hale-Bopp's dust production parameter, Afρ, was $2.0 \pm 0.8 \times 10^5$ cm when the comet was 2.33 AU from the Sun. Further, we find that its water production rate, Q_{H_2O}, was $2.6 \pm 0.4 \times 10^{29}$ s^{-1}. Combining this result with both other published H_2O production rates and CO production rates, we find that our measurements were made at the begining of the period when the comet's activity was transitioning from a H_2O-dominated to a CO-dominated state. We also find that the average rate of decrease of the water production between perihelion and 2.33 AU post perihelion was very close to $r_h^{-4.0 \pm 0.6}$, but concerns over radio data indicate that it may have been shallower immediately post-perihelion and then considerably steeper beyond about 2 AU. Such a behavior could indicate a sharply declining H_2O production rate beyond 2 AU, but if this is the case, then the H_2O production curve's steepening and turn-off occurred ≈1 AU closer to the Sun post-perihelion than did the H_2O turn-on pre-perihelion. An alternative explanation could be that a seasonal (i.e., obliquity-dependent shadowing) effect may have caused a reduction in illuminated area on Hale-Bopp's irregular nucleus between 1.5 and 2.3 AU outbound.

1. INTRODUCTION

The study of comets in the ultraviolet has been a highly productive pursuit (e.g., Feldman 1982; Feldman 1991; Festou et al. 1993; Stern 1999). Comet Hale-Bopp (C/1995 O1) presented solar system astronomers with a spectacular opportunity to study a high-activity comet in this way. We took advantage of this opportunity by proposing to fly our UV imager, the Southwest Ultraviolet Imaging System (SWUIS; see Slater et al. 1999), aboard the Space Shuttle. The primary objective of this mission was to provide a unique set of OH and UV continuum measurements by observing Hale-Bopp at some point during the long, almost 9 month period surrounding the comet's 1 April 1997 perihelion, when the comet would be at too small a solar elongation angle (SEA) to be observed by UV instruments aboard the Hubble Space Telescope (HST).

Although not specifically designed for cometary observations, SWUIS has certain attributes that make it useful for this purpose; these include a comparatively wide FOV (adjustable from 0.1 to 0.6 deg with the telescope; up to 12 deg can be achieved using a lens instead of the telescope), high temporal resolution (60 Hz), and the capability to observe objects at SEAs as low was 17 deg.[1]

SWUIS flew its first mission aboard STS-85 in early August of 1997, with the objective of obtaining images of Hale-Bopp in various bandpasses from 2500–8500 Å. The experiment performed flawlessly, and some 4.3×10^5 images of the comet were obtained. Here we report our first results. These involve a small fraction of the SWUIS dataset, centering on the

---

[1] SWUIS was in fact designed, and was initially selected, to fly on the Shuttle to obtain photometry and spectroscopy of Venus, Mercury, and the Jovian system; these observations have been delayed owing to Shuttle scheduling, but are now to begin in July, 1999 aboard STS-93.

determination and interpretation of H_2O and dust production measurements of the comet at 2.3 AU. Future reports are planned once more analyses have been completed, with the intent of exploring OH and continuum band image morphologies, and color-dependent Afρ measurements.

2. INSTRUMENT OVERVIEW

SWUIS is a mid-UV/VIS instrument capable of imaging astronomical targets in any filter bandpass throughout the 2500 Å to 8500 Å region.[2] The imager+electronics system is fed by an 18-cm aperture, fused silica/MgF_2 UV-Maksutov telescope with an adjustable focal length (1.05 to 2.57 m). The telescope feeds an optical coupler capable of housing up to 3 filters in series, which in turn feeds one of two image-intensified CCDs (ICCDs). The two ruggedized SWUIS ICCDs are sensitive to the visible (>30% DQE 4000–8500 Å, peak at 6500 Å) and the UV (>20% DQE 2000–6500 Å, peak at 3500 Å). The cameras can operate in either manual or automatic gain modes, and have a 370x420 pixel format. The ICCDs frame at 60 Hz, allowing us to co-register and coadd images to remove low-level attitude deadband jitter and drift. SWUIS data are recorded using a standard, on-board Shuttle video interface; data can also be transmitted to the ground in real-time for diagnostic purposes. Filters can be changed out to select various bandpasses, as desired.

SWUIS is specifically designed to operate as a Shuttle in-cabin instrument. The Shuttle cabin has 10 windows; of highest utility is the optical-quality UV-transmissible window on the Middeck of each vehicle. This window has >70% transmission from 2200 Å to almost

---

[2] Flights 2 and 3 will enhance these capabilities by extending the bandpass to 1.1 μm, doubling sensitivity, adding a sub-arcsecond high-resolution mode, and adding a long-slit, Rowland circle spectrograph facility.

2 μm. SWUIS observations are obtained by dedicated pointings scripted into the Shuttle's attitude timeline. Coarse pointing is achieved through Shuttle attitude control and fine pointing is adjusted via a pivot joint in the instrument's two-axis window mount.

3. HALE-BOPP OBSERVATIONS AND DATASET

SWUIS was launched aboard the Shuttle Discovery on 8 August 1997.[3] The mission extended over 1997 August 8–17. SWUIS imaging runs were obtained on August 9, 12, 14, and 15. The mean heliocentric distance, heliocentric velocity, and geocentric distance of Hale-Bopp at the time of the observations were 2.33 AU, 21.4 km sec^{-1}, and 2.93 AU, respectively. The image plate scale selected for the Hale-Bopp observations maximized the FOV (ϕ=3D0.6 deg) at the expense of spatial The data have been frame-grabbed for the analysis that follows in a 320x240 pixel format, yielding an effective scale of 8.7 arcsec/pixel, or 1.86$\times$10^4 km/pixel in the plane of the sky.

SWUIS observed comet Hale-Bopp on 9 orbits during STS-85. The timing and content of these 9 SWUIS data takes are summarized in Table 1. The filters used were primarily those contained in the standard Hale-Bopp filter set (see Millis et al. 1997; Farnham & Schleicher 1999; see also `http://www.lowell.edu/users/farnham/hb/hbfilters/index.html`).

In what follows we consider only the OH data obtained on 1997 August 12 and the clear filter continuum images (λ_c=3D5450Å) obtained on 1997 August 16. These include some 6,000 OH frames, which we coadded for analysis of the comet's water production rate, Q$_{H_2O}$, and some 20,000 broadband continuum frames, which we combined to obtain a measure of the comet's dust production. Figure 1 depicts a sample of unprocessed continuum data.

---

[3] Originally, we had hoped to conduct these observations near perihelion at the end of March 1997, but Shuttle programmatic constraints precluded that possibility.

4. DATA REDUCTION

As noted previously, SWUIS data frames are taken at a 60 Hz rate. This data stream is later spatially co-registered, and then coadded to enhance S/N. Background stars in the frames are used to accurately co-register the images. As a part of the coaddition process, the data are median filtered in small groups (during which image jitter is negligible) to remove video noise. Video banding is removed via a combination of FFT filtering and removing the average background trend in the image along each axis. Instrumental dark counts, determined in flight with a dark slide, were subtracted from each coadded image. Each resulting coadd in a given filter bandpass was then flat fielded using a laboratory flat field determined by measurements of a uniformly illuminated flat screen.

The effective sensitivity of any given SWUIS observation depends both on the instrument response and the Shuttle UV window transmission. Because this window obtains a thin film resulting from launch debris and space exposure, it is preferable to employ an in-flight calibration to a laboratory calibration pre- or post-flight. Instrument sensitivity was therefore measured in flight by comparing image counts for background stars of known spectral type and distance identified in the images, to their estimated flux in the filter bandpass used for the given observation. Background-subtracted stellar flux in a given image coadd was measured using standard aperture photometry techniques. Calibration stars were identified using the on-line SIMBAD star catalog. We relied on HD 59934 for the OH data (B2III/IV, m_V=3D8.0) and HD 60626 for the continuum data (G3/G5V, m_B=3D9.6), and normalized their known magnitudes and reddening to Kurucz models (Kurucz 1992) for each star. We point out that because SWUIS measurements are made above the Earth's atmosphere, flux uncertainties due to atmospheric absorption of the stellar spectral energy distribution are zero.

5. DERIVED DUST MEASURE

We now turn to the subject of Hale-Bopp's dust production at 2.33 AU, using the $Af\rho$ formulation as a measure (A'Hearn et al. 1984):

$$Af\rho =3D \left(\frac{F_{\rm comet}}{F_{\odot}}\right)\left(\frac{2r_h\Delta}{\rho}\right)^2 \rho \qquad (1)$$

Here, $F_{\rm comet}$ is the flux received from the comet by the instrument, $F_{\odot}$ is the solar flux at 1 AU convolved with the effective transmission function of the instrument, r_h is the comet's heliocentric distance (in AU), ρ is the radius of integration of the continuum flux, and Δ is the geocentric distance of the comet.[4]

We calculated the $Af\rho$ result from the coaddition of 20,000 broad (2500–8500 Å) bandpass images, assuming all of the light (after background subtraction) is due to the continuum (i.e., dust). Since Hale-Bopp was particularly dusty, this is a good approximation, but is, strictly speaking, an overestimate by a factor of ≈10%. The comet flux was obtained by integrating over a circular field of view centered on the comet superimposed on the image, with a radius of 5 pixels, corresponding to ρ=3D9.20×10^4 km.

We derive log(Afρ cm)=3D5.30±0.15 when Hale-Bopp was 2.3 AU from the Sun, a record among all comets at this distance. The Weaver et al. HST team found log(Afρ cm)=3D5.09±0.2 at 1" from the comet and at an effective wavelength of 6500Å, when Hale-Bopp was 2.48 AU from the Sun. These two results are in excellent agreement, and reconfirm the high dust production of comet Hale-Bopp. Typical long-period comets have

---

[4] We note that the user of Eqn. (5.2) must be careful, in that whereas the units on r_h must be in AU, the units in Δ/ρ can be anything, so long as they are homogenous; then the second ρ outside the parenthesis sets the units for Afρ itself.

log(Afρ cm) values in the range 2.5 to 4 (A'Hearn et al. 1995); in the next section, after deriving the water production rate for Hale-Bopp at 2.33 AU, we compare its log(Afρ/Q_{H_2O}) to other comets.

6. DERIVED H_2O PRODUCTION RATE

We used the vectoral model (Festou 1981) to derive water production rates from the OH 0–0 band brightness (see also Budzien et al. 1994). In the model, the lifetimes at 1 AU for H_2O (86,280 s total, 116,300 s dissociative) and OH (142,000 s total) were calculated for the solar activity level for August 1997, according to the procedure described in Budzien et al. (1994). The solar minimum OH (0–0) zero velocity g-factor at 1 AU was corrected to Hale-Bopp's heliocentric velocity (see Schleicher & A'Hearn 1988),[5] yielding 9.4×10^{-4} s^{-1}; this 1 AU value was then propagated to the heliocentric distance of Hale-Bopp. The value of Hale-Bopp's H_2O parent velocity determined by Colom et al. (1999), v_p=3D1.045$\sqrt{r_h}$ km s^{-1}, was adopted for the model calculations presented below.[6]

The comet center was located in OH from the 2-D moments of the center of light around the cometary emission peak. The average OH brightness was calculated over the central 5 by 5 pixels (43"x43"). A background level was determined for the data using an average value of image brightness measured far in the anti-solar direction from the comet. By scaling the measured-continuum flux to the OH flux, and adjusting for both the relative

---

[5] This g-factor has the same value for the quenched and unquenched cases; Schleicher, priv. comm.

[6] In contrast, Weaver et al. (1999) used a parent velocity of v_p=3D0.80$\sqrt{r_h}$ km s^{-1} in their analysis of small-FOV HST data. adopting our v_p relation would reduce the Weaver water production rate values by the factor 0.8/1.045=3D0.766.

equivalent widths of the two filters and the integrated solar flux in each filter, one easily derives that the continuum contribution to the OH band images of Hale-Bopp must be at or below the 4% level, and can be neglected for our purposes.

The observed OH brightness is 6.7±1.1 kR in the coadded images. This brightness yields optically thin column densities, from which we derived Q_{H_2O}=3D2.6±0.4×10^{29} molecules s^{-1} at 2.33 AU. This value is in very close agreement with the Q_{H_2O}=3D2.4±0.2×10^{29} s^{-1} obtained later by Weaver et al. (1999) using HST when Hale-Bopp was at a heliocentric distance of 2.48 AU; indeed, the agreement is so close, given the estimated error bars and the difference in Hale-Bopp's heliocentric distance, that the degree of formal agreement appears remarkable indeed.

In agreement with Weaver et al. (1999), our H_2O sublimation model estimates indicate that between 2% and perhaps 20% of Hale-Bopp's nucleus was actively releasing water, depending on the assumed temperature distribution on the surface; active fractions >5% are rare in comets (A'Hearn et al. 1995).

We now turn to the "big picture" view that the various datasets imply about Hale-Bopp's post-perihelion behavior. Figure 2 shows both the SWUIS and HST Q(H_2O) post-perihelion measurements, as well as the radio determinations of Q(H_2O); Figure 2 also shows pre-perihelion Q(H_2O) data derived from radio measurements. With regard to Q(H_2O), notice that the only post-perihelion radio observations (λ=3D18 cm) yielded H_2O production rates of 3.5×10^{30} s^{-1} and 2.1×10^{30} s^{-1} at 1.64 and 1.84 AU, respectively (Colom et al. 1999); Hale-Bopp moved rapidly southward thereafter, and no further radio measurements were made.

Combining our Q(H_2O) results with the perihelion water production rate of 1.2±0.9×10^{31} for Hale-Bopp (Colom et al. 1999), as shown in Figure 2, we find that the average rate of decrease of the water production between perihelion and 2.33 AU post perihelion is about $r_h^{-4.0\pm0.6}$; a similar analysis using the HST data obtained at 2.48 AU gives $r_h^{-3.8\pm0.3}$. Hale-Bopp's average post-perihelion rate of decrease of water production, derived from these two results, is thus quite typical of that observed in other old, long-period comets (A'Hearn et al. 1995), which have an average of $r_h^{-3.77}$. The fact that Hale-Bopp's water production rate decrease is typical gives a strong indication that Hale-Bopp's nucleus was not entirely outgassing.

One interesting point about the Q(H_2O) values is that they are very comparable to the Q(CO) values derived by submillimeter techniques in a similar range of r_h (Colom et al. 1999), indicating that Hale-Bopp's activity evolved from being H_2O-dominated inside ≈2.5 AU to CO-dominated beyond 3.5 AU (see Figure 2; compare the blue-line, post-perihelion Q(CO) data to the thick red line depicting Q(H_2O)). It is also interesting to note that pre-perihelion, the CO-to-H_2O activity evolution occurred about 1 AU farther out, near 3.4 AU (Biver et al. 1997), as shown in Figure 3.

However, inspecting the thick red line in Figure 2, one sees that in order to connect the post-perihelion radio and UV points, one requires a distinct change in the water production rate dependence on heliocentric distance somewhere between 1.6 and perhaps 2.0 AU. To make this finding more quantitative, notice that from perihelion through 1.84 AU 18 cm radio measurements correspond to an H_2O production falloff rate of $r_h^{-2.3\pm0.3}$; to accommodate these points with the SWUIS and HST UV data, the decline in H_2O production of Hale-Bopp must have then steepened to a value near $r_h^{-7.2\pm0.6}$ as the comet moved outward to 2.4 AU.[7]

---

[7] We note that Weaver et al. (1999)'s pre-perihelion results do show that the HST (UV) water production rates are systematically below the radio results inside 3 AU, thereby leading to the conclusion that some might find it not unexpected that post-perihelion UV-derived Q(H_2O) results would also fall below the radio-derived Q(H_2O) results.

What could this mean? Such a steepening of the water production rate might be expected at the time of the H_2O production turn off, but we must note that if this is the cause, then as shown by Figure 3, the H_2O production curve's steepening and turn-off occurred ≈1 AU closer to the Sun post-perihelion, than did the H_2O turn-on pre-perihelion.

One alternative physical mechanism could be a seasonal (i.e., obliquity-dependent shadowing) effect which may have caused a reduction in active area on Hale-Bopp around the time it reached 1.6–1.8 AU.

Another possibility is that the radio-derived Q(H_2O) points at 1.64 and 1.84 AU may be high owing to uncertainties in the OH inversion parameter i (see Despois et al. 1981) used by Biver et al. (1999). For comparison, Biver et al. used the value i=3D0.03 (calculated by Schleicher & A'Hearn 1988), but Colom et al. (1999) used Despois's higher value of i=3D0.13; Festou & Zucconi (pers. comm.) have independently calculated i=3D0.06 for the same heliocentric velocity, +21 km s^{-1}. Proportionately higher values of i lower Q(H_2O) proportionately; so, for example, i=3D0.13 would lower the radio-derived Q(H_2O) values by a factor of almost 4, which would make the radio-derived results consistent with a single-valued power law from perihelion all the way to the two UV-derived Q(H_2O) determinations.

7. CONCLUSIONS

We obtained a large dataset of visible and UV images of comet Hale-Bopp using the SWUIS UV/VIS imager during Space Shuttle mission STS-85 in August of 1997. At this time the comet was 2.33 AU from the Sun and at a solar elongation angle that prevented other UV (and indeed many visible) instruments from obtaining data. These measurements were made at a time when the H_2O and CO production rates were comparable.

In this report, we have described the SWUIS instrument, its Hale-Bopp dataset, and derived H_2O and dust production measures obtained from these data. We found that Hale-Bopp's dust production parameter, Afρ, was $2.0\pm0.8\times10^5$ cm when the comet was 2.33 AU from the Sun. Further, we found that Hale-Bopp's Q_{H_2O} was $2.6\pm0.4\times10^{29}$ s^{-1} at this point. We found from the Q_{H_2O} determination, that between 2% and 20% of Hale-Bopp's nucleus was active at any given time.

The SWUIS- derived log(Afρ/$Q_{\rm OH}$)=3D-24.1 shows that Hale-Bopp continued to be highly dusty (by a factor of order 10 to 20) compared to typical comets (see A'Hearn et al. 1995), both in absolute terms, and compared to its water production rate, as it receded from the Sun and its activity declined. Comparing the dust/water production ratio at the time of our post-perihelion measurements to a similar result obtained pre-perihelion at 2.48 AU (Schleicher & Farnham 1997), we find that in absolute terms, the comet was releasing about as as much dust pre- and post-perihelion, but that in relative terms the comet was dustier post-perihelion at 2.3 to 2.5 AU, than in the same heliocentric range pre-perihelion, owing to reduced water production.

Together, our Q_{H_2O} determination and the one made by HST at 2.48 AU demonstrate that either the radio-derived Q_{H_2O} results shown in Figure 2 are too high, or that the comet's behavior changed, owing to seasonal or other effects that caused its water production rate to begin declining more steeply after ≈1.8 AU.

We thank Bill Tomlinson, Tom Booker, and Don Mahoney at SwRI, Richard Sturtz of Xybion, Inc., and Vic Genau for their diligent attention to detail and care in building and qualifying SWUIS for flight. We thank Al Ong, Jackie Prewitt, Barbara Smith, and the entire JSC flight control team for their great help in planning and executing the SWUIS observations. We also wish to thank the entire STS-85 flight crew for conducting the actual observations of Hale-Bopp with SWUIS. Both referee David Schleicher and Dan

Durda provided helpful critiques of this manuscript. This work was supported by NASA's Office of Space Science under the Planetary Astronomy and Suborbital Research Program (NAG5-5098), NASA Planetary Astronomy grant NAG5-7312, JPL contract 960549, and JHU/APL contract 759577.

REFERENCES

A'Hearn, M.F., Schleicher, D.G., Feldman, P.D., Millis, R.L., and Thompson, D.T., 1984. *AJ*, **89**, 589–602.

A'Hearn, M.F., Millis, R.L., Schleicher, D.G., Osip, D.J., and Birch, P.V., 1995. *Icarus*, **118**, 223–270.

Biver, N., et al., 1997. *Science*, **275**, 1915–1918.

Biver, N., et al., 1999. *Earth, Moon, & Planets*, in press.

Budzien, S.A., Festou, M.C., and Feldman, P.D., 1994. *Icarus*, **95**, 65–72.

Colom, P., Gérard, E., Crovisier, J., Bockelée-Morvan, D., Biver, N., Rauer, H., 1999. *Earth, Moon, Planets*, in press.

Despois, D., Gerárd, E., Crovisier, J., and I. Kazes, 1991. *A&A*, **99**, 320–340.

Farnham, T. L., and Schleicher, D. G. 1999, Icarus, submitted

Feldman, P.D., 1982. In *Comets* (L.L. Wilkening, ed.) U. Az. Press, Tucson, 461–479.

Feldman, P.D., 1991. In *Comets in the Post-Halley Era* (R. Newburn, M. Neugebauer, & J. Rahe, eds). Dordrecht:Kluwer. p. 141–148.

Festou, M.C., 1981. *A&A*, **96**, 69–79.

Festou M.C., Rickman H., and West R., 1993. A&A Revs., 4, 363–447 and 5, 37–163.

Kurucz, R.L., 1992. In *The Stellar Populations of Galaxies* (eds. B. Barbuy & A. Renzini), IAU 149, Dordrecht: Kluwer, p. 225–232.

Millis, R., Schleicher, D.G., and Farnham, T., 1997. *BAAS*, **29**, 1035.

Schleicher, D.G., and A'Hearn, M.F., 1988. *ApJ*, **331**, 1058–1077.

Schleicher, D.G., and Farnham, T., 1997. *Science*, **275**, 1913–1915.

Slater, D.C., S.A. Stern, W.M. Tomlinson, D.E. Mahoney, J.Wm. Parker, P.M. Tamblyn, W.B. Colwell, D.D. Durda, P.R. Weissman, & F. Vilas, 1999. In *Proc. Space Technology and Applications International Forum (STAIF-99)*, Albuquerque, NM, in press.

Stern, S.A., 1999. In *The Origin and Composition of Cometary Material* (K. Altwegg, P. Ehrenfreund, J. Geiss, & W. Huebner, eds.). International Space Science Institute (ISSI), Bern, Switzerland. In press.

Weaver, H.A., Feldman, P.D., A'Hearn, M.F., Arpigny, C., Brandt, J.C., and Stern, S.A., 1999. *Icarus*, in press.

Woods, T.N., Prinz, D.K., London, J., Rottman, G.J., Crane, P.C., Cebula, R.P., Hilsenrath, E., Brueckner, G.E., Andrews, M.D., White, O.R., VanHoosier, M.E., Floyd, L.E., Herring, L.C., Knapp, B.G., Pankratz, C.K., and Reiser, P.A., 1996. *JGR*, **101**, 9541–9569.

This manuscript was prepared with the AAS LaTeX macros v4.0.

Table 1: SWUIS Hale-Bopp Observation Summary

SWUIS Orbit	Date	Imaging Filters
STS-85-1	09 Aug 1997	Green Continuum, OH, H_2O^+, CO^+
STS-85-2	09 Aug 1997	CS, UV continuum, C_2, CN, OH
STS-85-3	12 Aug 1997	OH, CN, C_2, Broadband Vis continuum
STS-85-4	12 Aug 1997	Broadband UV, H_2O^+
STS-85-5	14 Aug 1997	OH, UV continuum, Broadband Vis continuum
STS-85-6	14 Aug 1997	OH, UV continuum, Broadband Vis continuum
STS-85-7	14 Aug 1997	OH, CN, C_2, Broadband Vis continuum
STS-85-8	15 Aug 1997	OH, UV continuum, Broad-Band Vis continuum
STS-85-9	15 Aug 1997	OH, UV continuum, Broad-Band Vis continuum

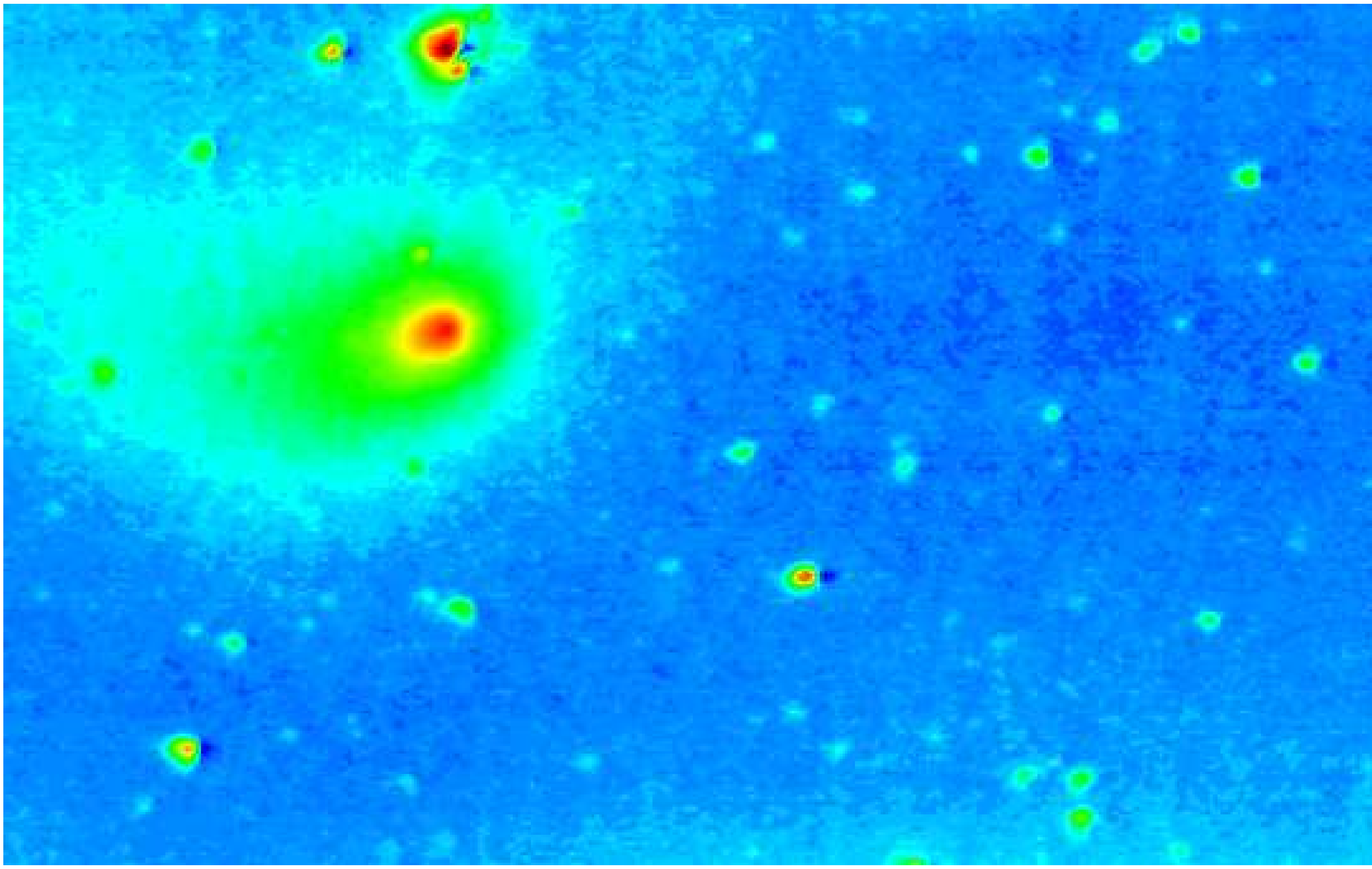

Fig. 1.— A direct coadd of 30 seconds of SWUIS Hale-Bopp data made with the clear filter on 13 Aug 1997. The field shown measures 0.45x0.34 deg, and represents a "raw" data product: the 1800 images used in this coaddition were not coregistered during coaddition, and the resulting image has neither been calibrated nor flat fielded. In addition to Hale-Bopp (total visual magnitude 4.7), field stars as faint as V=3D11.5 are also visible here.